



Research Article

Comparison of thermal response times of historical and modern building wall materials

Ahmet YÜKSEL^{1,2}, Müslüm ARICI^{2,*}, Hasan KARABAY²

¹*Yalova University, Yalova Vocational School, Electric and Energy Department, Yalova, Turkey*

²*Kocaeli University, Engineering Faculty, Mechanical Engineering Department, Kocaeli, Turkey*

ARTICLE INFO

Article history

Received: 07 February 2020

Accepted: 05 July 2020

Key words:

Historical buildings; Thermal mass; U-Value; Indoor air temperature; Insulation; Lumped capacitance method

ABSTRACT

The study aims to identify the main reason of the thermal response time difference between historical and modern buildings. Therefore, in this study, the thermal response time of historical and modern wall structures and its effect on the interior air temperature change was investigated parametrically. Considering the environmental conditions of Kocaeli province, Turkey, the thermal response time of a historical building wall made of a cut stone was compared with those of brick and gas concrete wall structures having the same overall heat transfer coefficient using the second-order lumped capacitance approach. The insulation thicknesses of the three different construction materials for U-values of 0.6, 0.4 and 0.2 W/m²K were calculated and temperature variations of indoor environment, wall and insulation material were analyzed. In addition, the required thicknesses of insulation material to obtain the same heat transfer coefficients were determined in case of using the 0.1 m thickness of cut stone, brick and gas concrete structure materials. The maximum and minimum amplitudes of the inside air temperature were recorded as 0.59 and 0.18°C for the aerated concrete in Case 3 and for the cut stone in Case 2, respectively. As a result, the walls with high thermal inertia are less affected by the changes in the environmental temperature although their U-value is relatively high. For this reason, it can be stated that one of the reasons why historical buildings have thick walls is to increase thermal inertia and thereby improve thermal comfort by reducing energy loss.

Cite this article as: Yüksel A, Arıcı M, Karabay H. Comparison of thermal response times of historical and modern building wall materials. J Ther Eng 2021;7(6):1506–1518.

INTRODUCTION

Historical buildings are important structures that contain pieces of information about the history of humanity and the historic texture of the region. It is known that historical buildings such as museums, temples and libraries, which have come to the forefront with their unique

architectural structures, have generally thick walls. These wall structures are designed in a thick manner to maintain to ensure indoor air conditions suitable for human comfort in addition to static balance and aesthetical appearance. In the structures where domes are used, such as madrasah and caravanserai, the wall thickness increases as the loads

*Corresponding author.

*E-mail address: muslumarici@gmail.com

*This paper was recommended for publication in revised form by
Regional Editor Ali Celen*



Published by Yıldız Technical University Press, İstanbul, Turkey

Copyright 2021, Yıldız Technical University. This is an open access article under the CC BY-NC license (<http://creativecommons.org/licenses/by-nc/4.0/>).

(dome diameter, etc.) increase. For example, Izmit Pertev Pasha Mosque with a dome diameter of 16.75 m has a wall thickness of 203 cm [1]. In historical buildings, building wall materials vary according to the geographical locations and available underground resources of the region. Stone materials and derivatives are frequently encountered due to their many advantages, particularly easy availability. These materials, which were turned into building materials by handwork in history, have been used in wall construction in various geometries [2]. Today, stone building materials have been replaced by modern building materials such as brick and aerated concrete [3,4]. Performances of these materials are further improved using various additives such as rubber [5] and phase change material [6,7]. Besides, the insulation applications, improving the thermal performance of the wall, help to provide thermal comfort in the modern buildings by ensuring that inside conditions are less affected by changes in the outdoor environment [8,9].

There are many studies on the modern insulation materials and application of them on the modern buildings in the literature [10–12]. For instance, Nematchoua et al. [13] evaluated the effect of two types of wall material (concrete block and compressed stabilized earth block) on energy savings by calculating the optimum insulation thickness for a 22-year-old building in Cameroon. The optimum insulation thicknesses were obtained as 0.098 m for the concrete block and 0.095 m for the compressed stabilized earth block, and an energy saving of 79.8% was achieved for the optimum insulation thickness in the southern façade. Islam and Bhat [14] compiled literature studies on the thermal and acoustic insulation materials generated from textile wastes. It was stated that the insulating materials produced from textile wastes were eco-friendly and that recycled textile fibers had better properties than some insulating materials such as glass wool. Bottino-Leone et al. [15] analyzed the hydrothermal, energy and environmental performances of the six vegetal insulation materials. Due to the application of natural-based insulation, the importance of hydrothermal evaluation has come to the fore. It was determined that the external plasters used in general were unsuccessful in terms of rain protection and different waterproof external plaster materials should be used. Besides, it was concluded that vegetal materials are more sensitive to moisture accumulation which causes the deterioration of thermal performance rapidly. Finken et al. [16] examined the use of capillary active or hydrophilic insulation materials in order to solve the condensation problem caused by insulation application in buildings located in moist areas. In a study conducted in Denmark, where there are heavy rainfalls, mildew conditions were investigated by adding insulation materials (varying from 30 mm to 150 mm) to the bricks. The heat loss was reduced by approximately 85% with installing the vegetal insulation to both the inner and outer surfaces of the wall.

Beyond isolating modern buildings, there are also different studies carried out to reduce energy demands

without damaging the texture of historical buildings. Jerman et al. [17] evaluated the thermal performance and maximum dehumidification status of biological-based and traditional internal thermal insulation materials in historical and modern buildings. It was obtained that thermal conductivity of biological insulation materials was about 0.05 W/mK higher than that of conventional insulation materials. Murgul and Pukhkal [18] suggested to place insulation on the outer surface of historical buildings in the modernization process, in order to save higher amount of energy. They emphasized that this process should be done without disrupting the architectural aesthetics and considering possible condensation which may occur between the external plaster and the insulation. Lucchi et al. [19] examined the economic benefits of a historical wall using “The Cost Optimality Methodology”. In this context, the wall type and the insulation material were defined, the energy consumption was investigated depending on the position of the insulation material, optimum insulation thicknesses were calculated, and cost analyses were performed. When the cost of investment was considered, it was emphasized that insulation with glass wool was the most suitable choice.

The studies mentioned above mostly based on the non-transient analyses, i.e. the thermal capacity of the wall is not taken into consideration. There are also some studies concerned with the effect of the thermal capacity of the wall on the energy demand of modern buildings. The thermal inertia of a building wall can release and store heat depending on the temperature difference [20]. Al-Motawakel et al. [21] studied the relationship between the phase lags between the inner and outer surface of the wall for different thicknesses of brick, stone and concrete. It was reported that the phase lag was largest in the red brick, and smallest in the concrete, and it increased with the increase of material thickness. Aste et al. [22,23] examined the effects of different building elements with the same U-value on the thermal inertia and showed that buildings with high thermal inertia require about 10% less heating and cooling energy. Argunhan et al. [24] obtained more realistic dynamic behaviors by establishing relations between the thermophysical properties of building materials.

While the thermal capacitance of the walls has a significant impact on the energy demand and comfort conditions of modern buildings, they should have a much more significant impact on historical buildings as they have much thicker and heavier wall mass compared to the modern buildings. In the literature, no study was encountered regarding the thermal performance comparison of a thick-historic wall with a thin-modern wall structure. The thermal response time is one of the main parameters for such a comparison. The research scope and novelty of this study were to examine whether the main reason of the thermal response time difference between historical and modern buildings is the thermal conductivity of wall materials or the thermal mass of wall. With this purpose, the

effects of materials used in historical and modern buildings (namely, cut stone, brick and gas concrete) on the thermal response time and interior air temperature were analyzed in three different scenarios. A parametric numerical study was carried out for comparisons. The second-order lumped capacitance approach was employed to obtain the results due to the advantage of low computation cost without sacrificing the precision of simulation.

PROBLEM DESCRIPTION

In this parametric study, the outdoor weather conditions were obtained from the Meteorological Service of the Turkish State for Kocaeli province, Turkey, for September 2016 (Fig. 1). In order to facilitate the evaluation of the results, the study executed within three separate scenarios. The thickness of materials to meet the required U-values in the scenarios was given in Table 1. In the first scenario, the U-value of a historical building with a thick cut stone wall (1m) was taken into account as a reference case, and its performance was compared with the brick and aerated concrete walls (Fig. 2). The thicknesses of the brick and aerated concrete materials were adjusted to obtain the same overall heat transfer coefficient. In the second scenario, the effect of three different structural elements (cut stone, brick and aerated concrete) on the indoor air temperature was examined by using insulation material in order to provide the same U-value. In the last scenario, the thermal response time of insulated wall structures with relatively thinner main wall elements (0.1m) of all three structures was investigated. The considered U-values were 0.6, 0.4 and 0.2 W/m²K in Case 2 and Case 3 since the U-value of buildings should not exceed 0.6 W/m²K in Kocaeli which is located in the 2nd degree-day region of Turkey according to Turkish Standard, TS 825 [25,26].

It was assumed that the thermophysical properties of the structural materials were constant (Table 2). The considered room has dimensions of 5 m × 3 m × 3 m (width × height × length), i.e. the external wall surface of the room is

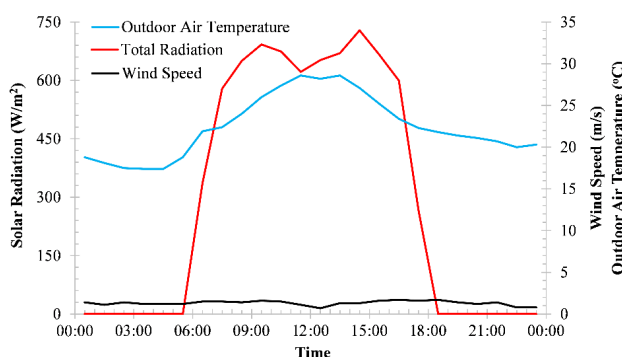


Figure 1. Outdoor environmental conditions data for Kocaeli province, September 2016.

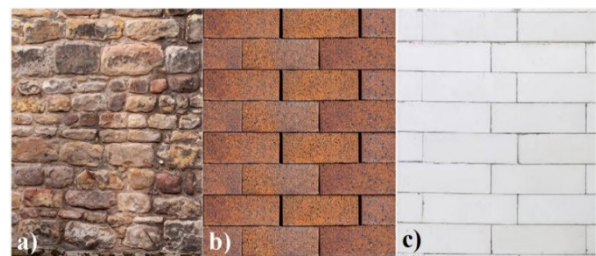


Figure 2. Considered building elements (a) cut stone [27] (b) brick [28] (c) aerated concrete [29].

15m² and the volume of the room is 45m³. The heat transfer coefficient between interior surface of the wall and indoor environment is 7 W/m²K.

NUMERICAL MODEL

In the literature, various numerical methods were used for the evaluation of thermal response time including lumped capacitance approach in buildings [30]. Crabb et al. [31] discussed the internal air temperature change in an intermittently used school with the lumped capacitance method. They showed that the numerical results overlapped with the experimental results. Kircher and Zhang [32] examined the accuracy of the lumped capacitance approach using a single capacitance on the wall. It was concluded that the approach can give accurate results even when the Biot number was greater than 0.1. Besides, they noted that the lumped system approach gave nearly exact results on the window glasses and acceptable outcomes on the walls. Therefore, it was decided to use the lumped capacitance approach in this study. With this aim, a program was developed in Fortran programming language.

The one-dimensional transient heat conduction equation is given as follows:

$$\frac{\partial T}{\partial t} = \alpha \frac{\partial^2 T}{\partial x^2} \quad (1)$$

The general energy balance equation used by considering the energy balance between the wall, internal and external environment in the lumped capacitance approach was given by Eq. 2 [33].

$$mc \frac{dT}{dt} = \sum Q_{in} - \sum Q_{out} \quad (2)$$

Two capacitances were installed in each main structural element. The capacitances were placed on the building element and indoor air when the insulation was not used (see Fig. 3a), and on the insulation material in addition to the building element and indoor air when the insulation was used (see Fig. 3b).

Table 1. The scenarios and parameters used

	U-Value (W/m ² K)	Material Type	Material Thickness (m)	Insulation Thickness (m)
Case 1	1.73	Cut Stone	1	–
		Brick	0.42	–
		Aerated Concrete	0.12	–
Case 2	0.6	Cut Stone	1	0.041
		Brick	0.42	0.041
		Aerated Concrete	0.12	0.041
Case 2	0.4	Cut Stone	1	0.073
		Brick	0.42	0.073
		Aerated Concrete	0.12	0.073
Case 3	0.2	Cut Stone	1	0.16
		Brick	0.42	0.16
		Aerated Concrete	0.12	0.16
Case 3	0.6	Cut Stone	0.1	0.061
		Brick	0.1	0.058
		Aerated Concrete	0.1	0.044
Case 3	0.4	Cut Stone	0.1	0.093
		Brick	0.1	0.089
		Aerated Concrete	0.1	0.076
Case 3	0.2	Cut Stone	0.1	0.188
		Brick	0.1	0.185
		Aerated Concrete	0.1	0.171

Table 2. Thermophysical properties of building materials

Type of Building Material	Thermal Conductivity (W/mK)	Density (kg/m ³)	Specific Heat (J/kgK)
Cut Stone	1.73	2050	1840
Brick	0.72	1920	835
Aerated Concrete	0.2	400	920
Insulation	0.038	32	840

In the Fig. 2, T_{out} is the outdoor temperature (°C), T_{in} is the indoor temperature (°C), T_w is the temperature of main building elements, T_{ins} is the temperature of insulation material. C_w , C_{in} and C_{ins} are the capacitance of wall, indoor and insulation, respectively. In calculating C_{ins} , it was taken into consideration that the air has a density of 1.184 kg/m³ and a specific heat of 1007 J/kgK and did not change with the temperature fluctuations in the interior air. R represents the total thermal resistances between the indicated temperatures in the wall. Also, L_w and L_{ins} stand for the thicknesses of the wall and insulation elements, respectively.

The thermal capacitances were calculated by Eq. 3.

$$C = \rho c_p V \quad (3)$$

The resistances indicated in the thermal network system in Fig. 2 are defined in Eqs. 4–8. As can be seen from these

equations, the total resistances were calculated for each section between outside ambient air and capacitances.

$$R_{out,1} = \frac{1}{h_{out}} + \frac{L_w}{3k_w} \quad (4)$$

$$R_{out,2} = \frac{1}{h_{out}} + \frac{L_{ins}}{2k_{ins}} \quad (5)$$

$$R_{in} = \frac{L_w}{3k_w} + \frac{1}{h_{in}} \quad (6)$$

$$R_{iw} = \frac{L_{ins}}{2k_{ins}} + \frac{L_w}{3k_w} \quad (7)$$

$$R_w = \frac{L_w}{3k_w} \quad (8)$$

Here, the subscripts of *out*, *in*, *w*, *ins* and *iw* represent outdoor, indoor, wall, insulation and insulated wall, respectively. The temperature distribution of the insulation, wall and interior air was obtained by Eqs. 9–15.

$$C_w \frac{dT_{w,1}}{dt} = \left(\frac{T_{out} - T_{w,1}}{R_{out,1}} - \frac{T_{w,1} - T_{w,2}}{R_w} \right) A_s \quad (9)$$

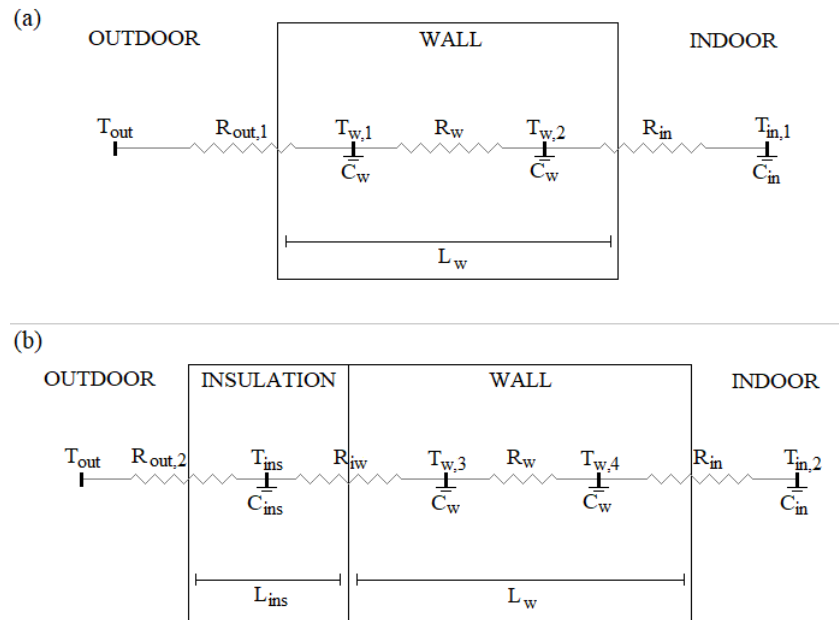


Figure 3. The capacitance and thermal resistance network for (a) Case 1 and (b) Case 2 and Case 3.

$$C_w \frac{dT_{w,2}}{dt} = \left(\frac{T_{w,1} - T_{w,2}}{R_w} - \frac{T_{w,2} - T_{in}}{R_{in}} \right) A_s \quad (10)$$

$$C_w \frac{dT_{w,3}}{dt} = \left(\frac{T_{ins} - T_{w,3}}{R_{iw}} - \frac{T_{w,3} - T_{w,4}}{R_w} \right) A_s \quad (11)$$

$$C_w \frac{dT_{w,4}}{dt} = \left(\frac{T_{w,3} - T_{w,4}}{R_w} - \frac{T_{w,4} - T_{in}}{R_{in}} \right) A_s \quad (12)$$

$$C_{ins} \frac{dT_{ins}}{dt} = \left(\frac{T_{out} - T_{ins}}{R_{out,2}} - \frac{T_{ins} - T_{w,3}}{R_{iw}} \right) A_s \quad (13)$$

$$C_{in} \frac{dT_{in,1}}{dt} = \left(\frac{T_{w,2} - T_{in,1}}{R_{in}} \right) A_s \quad (14)$$

$$C_{in} \frac{dT_{in,2}}{dt} = \left(\frac{T_{w,4} - T_{in,2}}{R_{in}} \right) A_s \quad (15)$$

The solar radiation was taken into account by the solar-air temperature [34,35]:

$$T_{sa}(t) = T_{out}(t) + \frac{\alpha_G S}{h_{out}} - \frac{\varepsilon \sigma (T_{out}^4(t) - T_{sky}^4)}{h_{out}} \quad (16)$$

where T_{sa} , T_{sky} , ε , S , α_G and σ are the solar-air temperature (K), sky temperature (K), emissivity, total radiation (W/m^2), absorptivity (0.6) and the Stefan-Boltzmann constant (5.67

$\times 10^{-8} \text{ W/m}^2\text{K}^4$), respectively. The exterior heat transfer coefficient (h_{out}) was calculated considering the wind speed (w , m/s) (Eq. 17) [36], and the sky temperature expressed in Eq. 16 was estimated by Eq. 18 [36].

$$h_{out} = 8.91 + 2w \quad (17)$$

$$T_{sky}(t) = 0.0552 T_{out}(t)^{1.5} \quad (18)$$

At this point, it is noteworthy to state that there are different opinions in the literature about the applicability of the lumped capacitance method for such problems depending on Biot number which represents the ratio between conductive resistance of a body and convective resistance at the surface of the object [37]. For instance, Xu et al. [38] suggested not to employ this method for problems involving large Biot number while Kircher and Zhang [32] claimed that it can be used with validation. Thus, a careful examination of Biot number was needed to verify the accuracy of this method. Considering the size and properties of the structural materials used in this study given in Table 1 and Table 2, it was found that the maximum Biot number is 3.6 for the aerated concrete material in Case 1 and Case 2 whilst the minimum Biot number is 0.2 for the cut stone building material in Case 3. Since all the Biot numbers were greater than 0.1 for the problem under investigation, the accuracy and validity of the lumped capacitance method were confirmed with the finite difference method as suggested in [39]. The one-dimensional transient heat conduction equation given in Eq. 1 was solved by an explicit finite difference method and the obtained results were compared with those of the first, second and third-order lumped capacitance

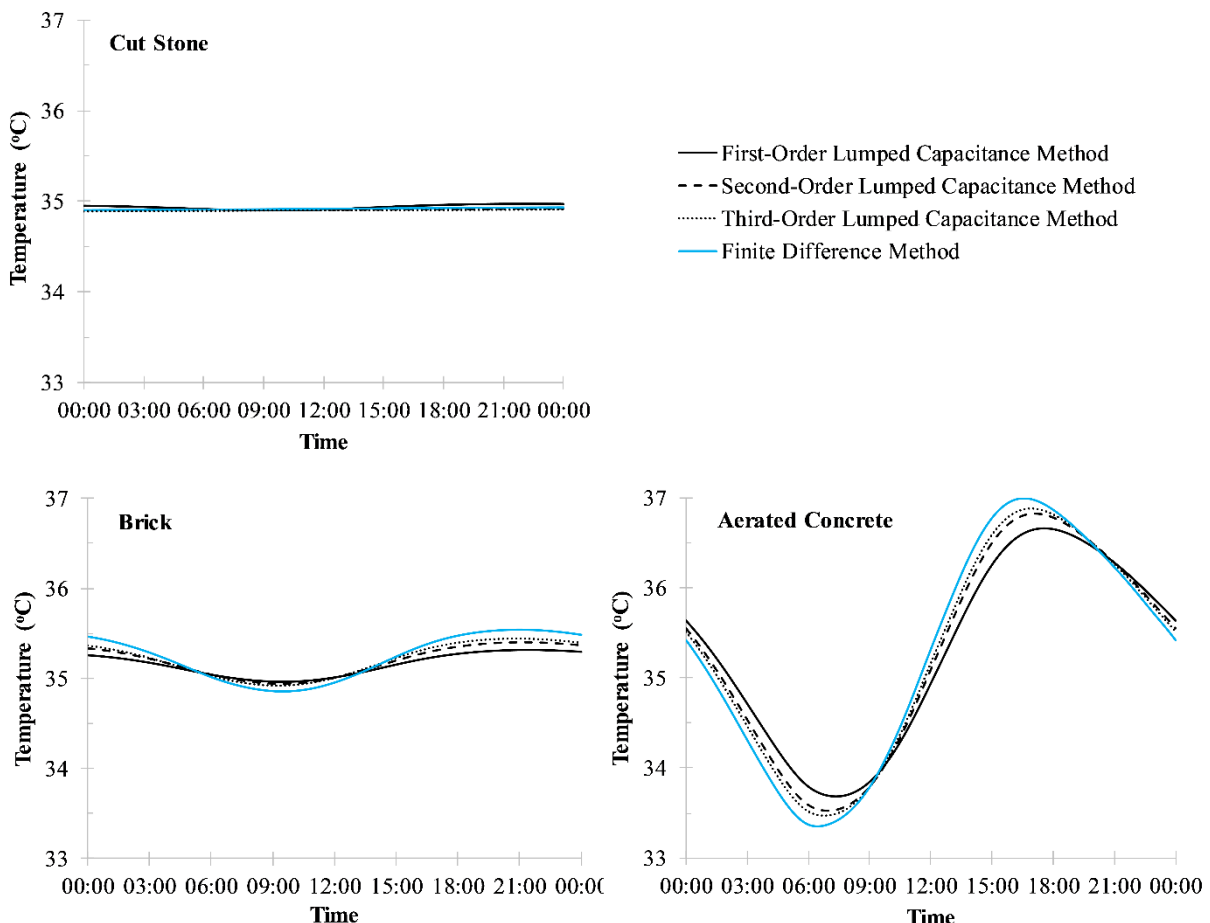


Figure 4. Comparison of interior air temperatures obtained by finite difference method and lumped capacitance approach with first, second and third order.

methods. At first, a mesh independent test was performed for the finite difference method considering the walls (cut stone, brick and aerated concrete) for Case 1 which has the largest Biot number. Then, the results obtained by the finite difference were used to assess the accuracy of the lumped capacitance methods. In the finite difference method, various equidistant meshes were tested, progressively increasing mesh density on the wall. It was observed that using 10 nodes on the wall is enough to provide mesh independent results. As seen in the Fig. 4, the interior air temperature for cut stone was around 35°C in all methods. The maximum difference between the interior air temperatures obtained by the first-order and second-order lumped capacitance method was 0.05°C, 0.09°C and 0.24°C for the cut stone, brick and aerated concrete, respectively. The maximum difference of interior air temperatures between the second-order and third-order lumped capacitance method was 0.01°C, 0.04°C and 0.08°C for the cut stone, brick and aerated concrete. In addition, the maximum temperature difference between the finite difference and the second-order lumped capacitance method was 0.01°C, 0.09°C and

0.29°C for the cut stone, brick and aerated concrete, respectively, which is in an acceptable range according to [40]. Therefore, the second-order lumped capacitance method was preferred for the further analysis due to its simplicity and low computation cost.

RESULTS AND DISCUSSION

In this study, thermal response times of wall structures of historical and modern buildings were compared for different scenarios. The effect of insulated and uninsulated conditions of thick historical and thin modern wall materials with the same U-value on the interior air temperature was investigated under three different cases. The results for each case are discussed below.

Case 1

A wall made of cut stone material with a thickness of 1m (U -value = 1.73 W/m²K) was considered due to the fact that the historical buildings have very thick walls. The thermal response time of this wall was compared with that

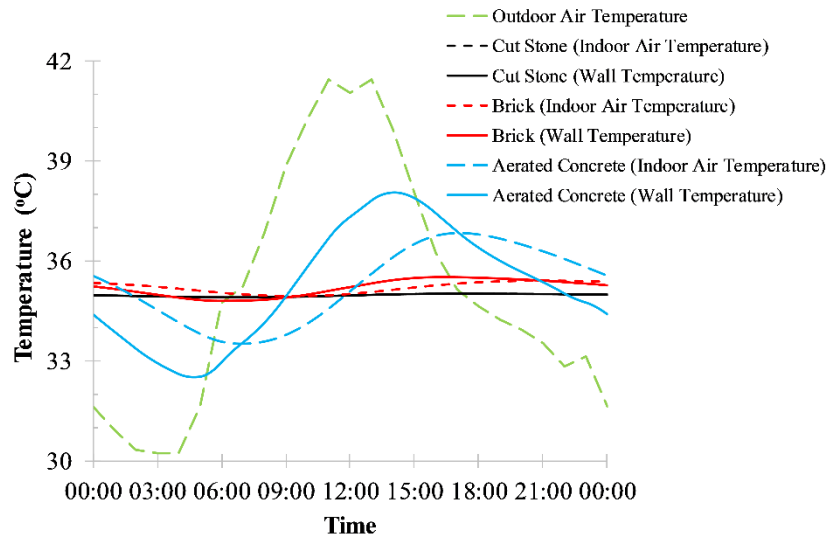


Figure 5. Variation of the indoor air and wall temperature for Case 1 (U -value = 1.73 W/m²K).

of the wall which have the same overall heat transfer coefficient formed from the brick and aerated concrete building materials used today. The thicknesses of uninsulated brick and aerated concrete walls to have the same U -value (1.73 W/m²K) were calculated as 0.42m and 0.12m, respectively. The temperature variation of the walls, which had the same U -value but made of different building materials along with resulting interior air temperatures were given in Fig. 5.

The outdoor air temperature change had an amplitude of 5.6°C, while the temperature fluctuations of the wall were 0.07°C, 0.35°C and 2.78°C for cut stone, brick and aerated concrete materials, respectively, and the temperature swings of the indoor air ambient were corresponding to 0.05°C, 0.23°C and 1.65°C. The temperature difference between outside and inside air temperatures at 13⁰⁰ was found to be 6.49°C, 6.36°C and 5.81°C, respectively, depending on the use of cut stone, brick and aerated concrete material. The cut stone had a much lower amplitude since its thermal mass was much higher than those of the other building materials with the same overall heat transfer coefficient. Furthermore, the lowest and highest amplitudes of the inside air temperatures were obtained in the cut stone and aerated concrete materials. Although the thermal conductivity of the cut stone material is higher compared to other building elements, the temperature differences between the wall and the indoor air have the lowest value since its thermal inertia is much higher than other materials. Conversely, although the thickness of the aerated concrete is much thinner than those of the other materials and its thermal conductivity is quite low, it has the highest value in temperature differences which caused the inside air temperature to be more affected by the outdoor environment. The obtained results were compatible with the results by Al-Motawakel et al. [21] in which similar properties of brick, stone and

concrete given were used, and also reported that the effect of outside temperature to reach the indoor environment was more delayed for the cut stone material compared to the aerated concrete.

Case 2

Kocaeli province is located in the 2nd degree-day region according to TS-825 standards [25]. The overall heat transfer coefficients in the buildings are required to be at most 0.6 W/m²K in this degree-day region. Using the material thicknesses given in Case 1 (1m, 0.42m and 0.12m for the cut stone, brick and aerated concrete, respectively), the insulation material (see Table 1) was added as required to meet the U -value. The insulation thickness was not changed according to the structure material since the U -values (1.73 W/m²K) of the main wall materials (cut stone, brick and aerated concrete) were the same. The insulation thickness was calculated as 0.041m, 0.073m and 0.16m for the U -value of 0.6, 0.4 and 0.2 W/m²K, respectively. The insulation was installed in the outer surface of the wall as suggested in [41]. The effects of the main structure and insulation materials on the interior air temperature were evaluated for the given outdoor environmental conditions.

The temperature variations of insulation and other wall materials for different U -values (0.6, 0.4 and 0.2 W/m²K) were given in Fig. 6. With the addition of insulation material to ensure the U -values of 0.6 W/m²K and below, the cut stone and brick structure materials were almost not affected by the external conditions. The temperatures of cut stone and brick structure materials remained almost constant at around 35°C, which swings between 34.87°C and 35.09°C, for all the considered overall heat transfer coefficients. Since the thinnest material (0.12m) was aerated concrete material, the temperature distribution had greater amplitudes than

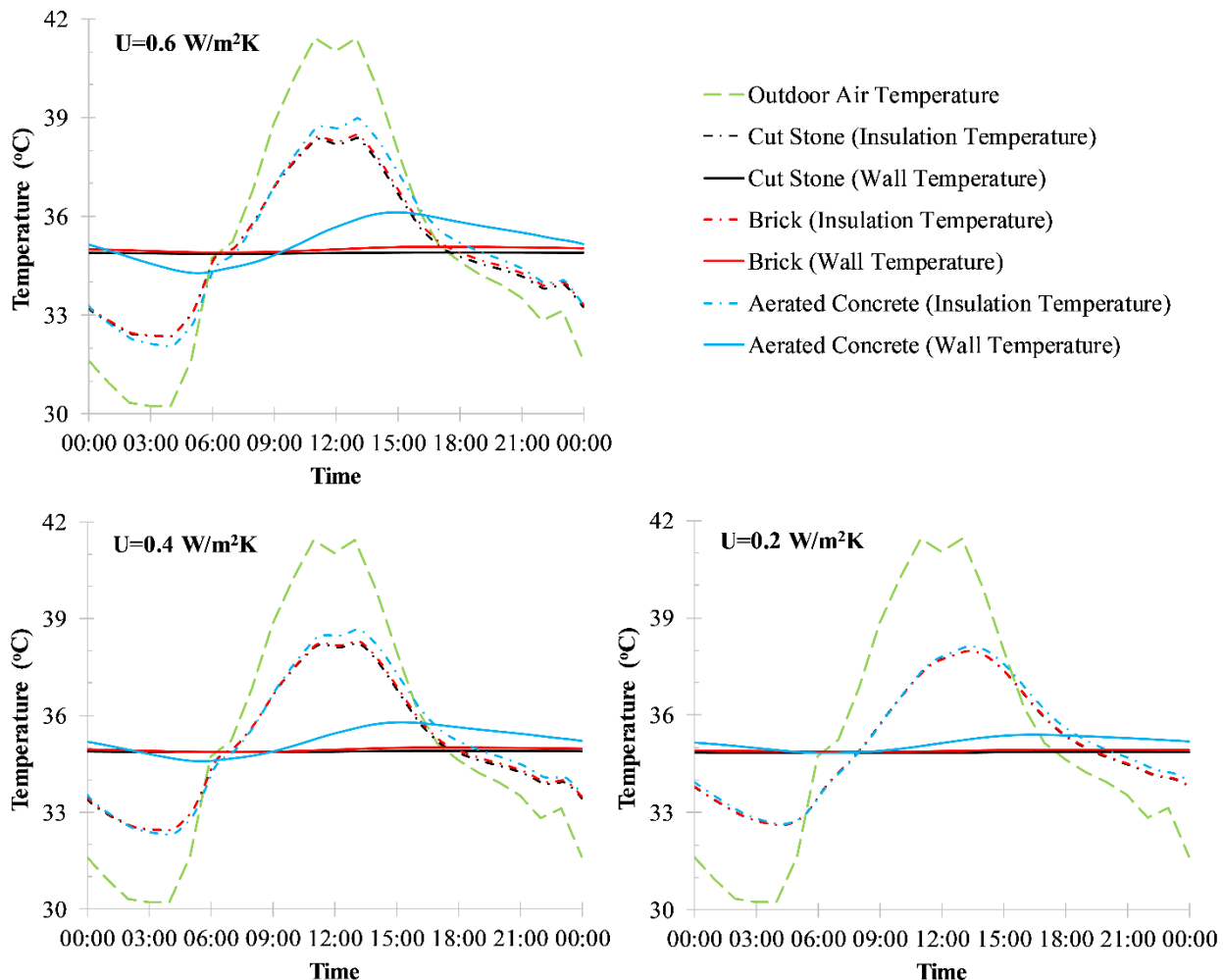


Figure 6. Temperature variation in different layers of wall for various U-values (Case 2).

other building elements. The temperature fluctuations in this structure material had an amplitude of 0.93°C, 0.61°C and 0.29°C, respectively, for $U = 0.6$, 0.4 and 0.2 $\text{W/m}^2\text{K}$. The largest temperature amplitudes of the insulation materials were obtained at the highest U -value (0.6 $\text{W/m}^2\text{K}$), which were 3.01°C, 3.06°C and 3.46°C, respectively, according to the use of the cut stone, brick and aerated concrete. The amplitude of the temperature fluctuations decreased as the U -value decreased and the lowest amplitudes were obtained at $U = 0.2 \text{ W/m}^2\text{K}$, which were 2.68°C, 2.69°C and 2.75°C for the cut stone, brick and aerated concrete, respectively. For all the main structure materials, the temperature fluctuation in the insulation material was higher compared to that of the wall temperature since the insulation was added to the outer surface. So, it can be stated that the insulation material absorbed the changes in the outside air temperature and damped down its effect on the wall. That is, the temperature variation of walls with higher mass is less influenced by the outdoor environment. A same observation was made by Argunhan et al. [24] which indicated

that wall materials with higher thermal storage capacity were less affected by the external environmental conditions.

Within the context of Case 2, the variation of interior air temperatures of different walls was presented in Fig. 7 for various U -values. When the U -value was 0.2 $\text{W/m}^2\text{K}$, the maximum interior air temperatures were 34.87°C, 34.93°C and 35.29°C for the materials of cut stone, brick and aerated concrete, respectively. For the cut stone, the interior air temperatures were nearly stable around 34.9°C. However, when the aerated concrete material was used, maximum amplitudes were obtained and an increase in the amplitude was observed due to the increase in the U -value. The maximum amplitudes were calculated to be 0.55°C, 0.37°C and 0.18°C, respectively, for the U -value of 0.6, 0.4 and 0.2 $\text{W/m}^2\text{K}$ for the aerated concrete. Furthermore, the minimum amplitudes were attained respectively for the $U = 0.6$, 0.4 and 0.2 $\text{W/m}^2\text{K}$ (for the cut stone). Since the decreases in the U -value caused the wall to be less affected by the outside air temperature changes, the temperature variation of the indoor air was observed to be exceptionally low.

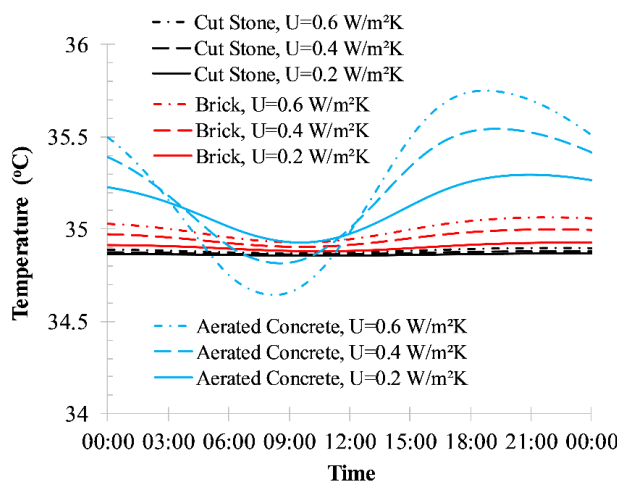


Figure 7. Variation in the inside air temperatures for different insulation thicknesses and wall materials (Case 2).

Case 3

In this scenario, the thermal response time was investigated regarding that the cut stone which is generally used in historical buildings was adapted to the modern buildings. The thickness of all materials (cut stone, brick and aerated concrete) was taken as 0.1 m thick, and the insulation thickness were varied to meet the desired U-values. The studied U-values were 0.6, 0.4 and 0.2 W/m²K. The required insulation thicknesses for different types of wall materials were presented above in Table 1 for different U-values.

The temperature fluctuations of insulation and other wall materials for different U-values (0.6, 0.4 and 0.2 W/m²K) and for different insulation thicknesses were plotted in Fig. 8. The maximum amplitude among the main structural elements was obtained as 0.94°C for the aerated concrete material for the largest U-value (0.6 W/m²K), as expected. Besides, the minimum amplitude was monitored as 0.04°C in the cut stone material for U = 0.2 W/m²K. As the U-value increased from 0.2 to 0.4 W/m²K or from 0.4 to 0.6 W/m²K, the wall temperature amplitudes of cut stone, brick and aerated concrete increased by 0.04°C, 0.09°C and 0.33°C, respectively. Since the insulation thickness was increased to reduce the U-value, the temperatures of the main wall component changed less with the decrease of the overall heat transfer coefficient. The maximum amplitude of the insulation temperatures was obtained as 3.4°C in the case of aerated concrete material with U = 0.6 W/m²K, the minimum amplitude was 2.47°C in the case of cut stone material with U = 0.2 W/m²K. The close trends of the insulation material to the characteristic of the outside air temperature were related to the increase of U-value, and the higher temperature amplitudes were observed as the insulation thickness decreased. Since the thermal conductivity of the cut stone building material was higher than other materials, the insulation

thickness was larger than the others. Therefore, the temperature of the insulation material on the wall made of cut stone material showed less variation compared to other situations. Furthermore, since a thinner insulation thickness was used for the aerated concrete wall, the insulation material had a more variable temperature distribution.

The influences of different structural elements (namely, cut stone, brick and aerated concrete) and different U-values (0.6, 0.4 and 0.2 W/m²K) on the indoor air temperatures for Case 3 were compared in Fig. 9. The maximum and minimum outside air temperatures were 41.5°C and 30.23°C while the maximum and minimum inside air temperatures were 35.79°C and 34.6°C, respectively, for the case of using the aerated concrete having a U-value of 0.6 W/m²K. The inside air temperature had a maximum amplitude (0.59°C) for the type of wall using an aerated concrete at U = 0.6 W/m²K, and a minimum amplitude (0.03°C) for the wall type using a cut stone at U = 0.2 W/m²K. As the U-value increased from 0.2 to 0.4 W/m²K and from 0.4 to 0.6 W/m²K, the amplitudes of inside air temperature for the cut stone, brick and aerated concrete increased by 0.03°C, 0.07°C and 0.2°C, respectively. As a result, it was observed that the internal environment was less affected by outdoor conditions in the structures with higher mass as reported in [42].

CONCLUSION

In this study, the effect of wall material of historical and modern buildings on the indoor air temperature was examined under various scenarios. Analyses were performed for the cut stone as a historical building material, and brick and aerated concrete materials as modern building materials under three different scenarios. In the first scenario (Case 1), the cut stone material with 1m thickness and with U = 1.73 W/m²K was taken as a reference, and the required thickness of the brick and aerated concrete materials were calculated to provide the same U-value. The effects of the main structure and insulation materials on the interior air temperature were examined for the given outdoor environmental conditions. In the second scenario (Case 2), the insulation material was added to the structural elements mentioned in Case 1 to obtain the U-value of 0.6, 0.4 and 0.2 W/m²K. In the third scenario (Case 3), the insulation materials of different thicknesses were added to 0.1m thick cut stone, brick and aerated concrete structural materials, such that U-values were 0.6, 0.4 and 0.2 W/m²K. The swing in interior air temperature was diminished for the cut stone with U = 0.2 W/m²K in Case 2, while the maximum variation which has an amplitude of 0.59°C was observed for the aerated concrete with U = 0.6 W/m²K in Case 3.

Consequently, it was found that in all cases, the cut stone wall material is less affected by the external environment, compared to other wall elements, due to its higher thermal mass. Thus, the minimum indoor air, wall and insulation temperature swings were attained by the cut stone building

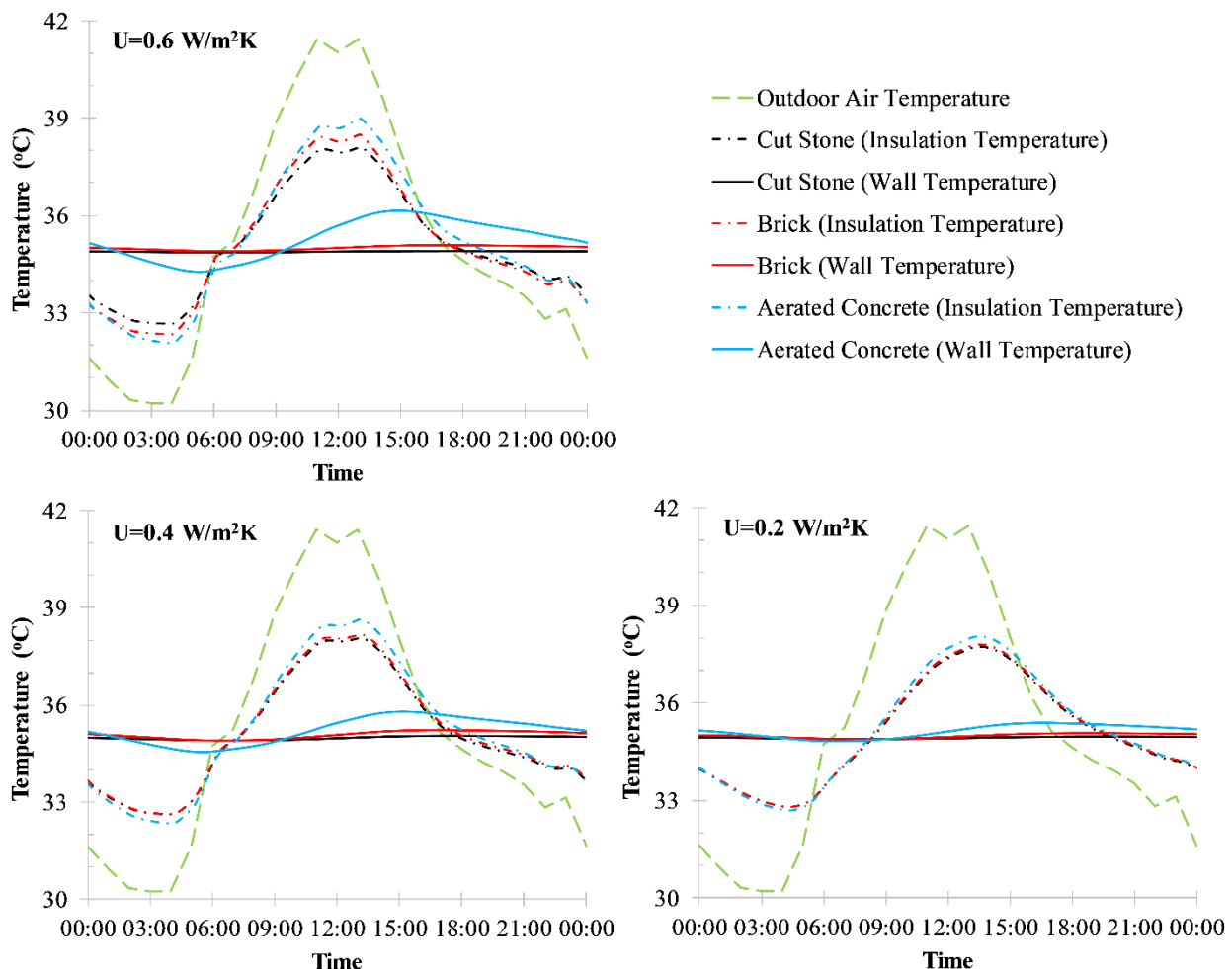


Figure 8. Temperature variation in different layers of wall for various U-values (Case 3).

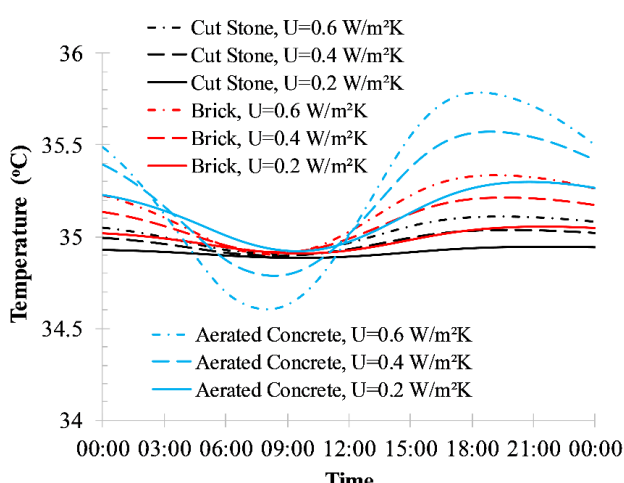


Figure 9. Variation of indoor air temperature for various insulation thicknesses and wall materials for Case 3.

material, which was followed by the brick material. The largest amplitudes in temperature changes were observed when the aerated concrete building materials were used. The differences in temperature amplitudes revealed that thermal mass must be taken into consideration along with the thermal conductivity for the selection of wall material and thickness (i.e. thermal resistance). It is worth to note that although the increase in thermal mass seems helpful in terms of reducing the temperature fluctuations (thus thermal comfort), it may cause more energy consumption as the wall should be cooled down or heated up together with the interior environment also. Therefore, a year-round analysis including both thermal mass and thermal conductivity of wall components should be performed to evaluate the thermal performance of buildings.

In conclusion, it can be said that the reason for the thick walls of the historical buildings is not only to build more durable structures against weight or external forces but also to reduce energy requirement and improve comfort conditions for the occupants in the indoor environment.

NOMENCLATURE

<i>A</i>	Area, m ²
<i>Bi</i>	Biot Number
<i>C</i>	Thermal capacity, J/K
<i>c</i>	Specific heat, J/kgK
<i>h</i>	Convection heat transfer coefficient W/m ² K
<i>k</i>	Thermal conductivity, W/mK
<i>L</i>	Thickness, m
<i>m</i>	Mass, kg
<i>R</i>	Thermal resistance, m ² K/W
<i>S</i>	Total radiation, W/m ²
<i>T</i>	Temperature, K
<i>U</i>	Overall heat transfer coefficient, W/m ² K
<i>V</i>	Volume, m ³
<i>w</i>	Wind Speed, m/s
<i>t</i>	Time, sec
<i>x</i>	Distance, m

Greek Symbols

α	Thermal diffusivity, m ² /s
ρ	Density, kg/m ³
ϵ	Emissivity
α_G	Absorptivity
σ	Stefan-Boltzmann constant, 5.67×10^{-8} W/m ² K ⁴

Subscripts

<i>in</i>	Refers to indoor
<i>ins</i>	Refers to insulation
<i>iw</i>	Refers to insulation and wall
<i>out</i>	Refers to outdoor
<i>s</i>	Refers to surface
<i>sa</i>	Refers to solar-air
<i>sky</i>	Refers to sky
<i>w</i>	Refers to wall

AUTHORSHIP CONTRIBUTIONS

Concept: AY, MA, HK; Design: AY, MA, HK ; Materials: AY, MA, HK ; Data: AY, MA Analysis: AY, MA, HK ; Literature search: AY, MA ; Writing: AY, MA, HK ; Critical revision: AY, MA, HK

DATA AVAILABILITY STATEMENT

No new data were created in this study. The published publication includes all graphics collected or developed during the study.

CONFLICT OF INTEREST

The author declared no potential conflicts of interest with respect to the research, authorship, and/or publication of this article.

ETHICS

There are no ethical issues with the publication of this manuscript.

REFERENCES

- [1] Spodek JC, Harrison CK. Cloud based 3-D digital photogrammetry Pertev Paşa Mosque (Izmit, Turkey). Conference: 3D Digital Documentation Summit At: New Orleans, LA, USA, April 2017.
- [2] Roca P, González JL, Oñate E, Lourenço PB. Experimental and numerical issues in the modelling of the mechanical behaviour of masonry. Structural analysis of historical constructions II. CIMNE, Barcelona. 1998:57–91.
- [3] Kalpana M, Mohith S. Study on autoclaved aerated concrete. Materials Today: Proceedings, 2020;22:894–896. [\[CrossRef\]](#)
- [4] Bruno AW, Gallipoli D, Perlot C, Kallel H. Thermal performance of fired and unfired earth bricks walls. Journal of Building Engineering 2020;28:101017. [\[CrossRef\]](#)
- [5] Turgut P, Yesilata B. Physico-mechanical and thermal performances of newly developed rubber-added bricks. Energy and Buildings 2008;40:679–688. [\[CrossRef\]](#)
- [6] Tunçbilek E, Arıcı M, Bouadila S, Wonorahardjo S. Seasonal and annual performance analysis of PCM-integrated building brick under the climatic conditions of Marmara region. Journal of Thermal Analysis and Calorimetry 2020;141:613–624. [\[CrossRef\]](#)
- [7] Korti AIN. Numerical simulation on the effect of latent heat thermal energy storage unit. Journal of Thermal Engineering 2016;2:598–606. [\[CrossRef\]](#)
- [8] Cui H, Overend M. A review of heat transfer characteristics of switchable insulation technologies for thermally adaptive building envelopes. Energy and Buildings, 2019;199:427–444. [\[CrossRef\]](#)
- [9] Abu-Jdayil B, Mourad AH, Hittini W, Hassan M, Hameedi S. Traditional, state-of-the-art and renewable thermal building insulation materials: an overview. Construction and Building Materials 2019;214:709–735. [\[CrossRef\]](#)
- [10] Villasmil W, Fischer LJ, Wörtschek J. A review and evaluation of thermal insulation materials and methods for thermal energy storage systems. Renewable and Sustainable Energy Reviews 2019;103:71–84. [\[CrossRef\]](#)
- [11] Anand Y, Anand S, Gupta A, Tyagi S. Building envelope performance with different insulating materials - An exergy approach. Journal of Thermal Engineering 2015;1:433–439. [\[CrossRef\]](#)
- [12] Ağbulut Ü. Mathematical calculation and experimental investigation of expanded perlite based heat

insulation materials' thermal conductivity values. *Journal of Thermal Engineering* 2018;4:2274–2286. [CrossRef]

[13] Nematchoua MK, Raminosoa CR, Mamiharijaona R, René T, Orosa JA, Elvis W, et al. Study of the economical and optimum thermal insulation thickness for buildings in a wet and hot tropical climate: case of cameroon. *Renewable and Sustainable Energy Reviews* 2015;50:1192–1202. [CrossRef]

[14] Islam S, Bhat G. Environmentally-friendly thermal and acoustic insulation materials from recycled textiles. *Journal of Environmental Management* 2019;251:109536. [CrossRef]

[15] Bottino-Leone D, Larcher M, Herrera-Avellanosa D, Haas F, Troi A. Evaluation of natural-based internal insulation systems in historic buildings through a holistic approach. *Energy* 2019;181:521–531. [CrossRef]

[16] Finken GR, Bjarløv SP, Peuhkuri RH. Effect of façade impregnation on feasibility of capillary active thermal internal insulation for a historic dormitory—A hygrothermal simulation study. *Construction and Building Materials* 2016;113:202–214. [CrossRef]

[17] Jerman M, Palomar I, Koci, V, Cerny R. Thermal and hygric properties of biomaterials suitable for interior thermal insulation systems in historical and traditional buildings. *Building and Environment* 2019;154:81–88. [CrossRef]

[18] Murgul V, Pukhkhal V. Saving the architectural appearance of the historical buildings due to heat insulation of their external walls. *Procedia Engineering* 2015;117:891–899. [CrossRef]

[19] Lucchi E, Tabak M, Troi A. The “cost optimality” approach for the internal insulation of historic buildings. *Energy Procedia* 2017;133:412–423. [CrossRef]

[20] Verbeke S, Audenaert A. Thermal inertia in buildings: A review of impacts across climate and building use. *Renewable and Sustainable Energy Reviews* 2018;82:2300–2318. [CrossRef]

[21] Al-Motawakel MK, Probert SD, Norton B. Thermal behaviors of vernacular buildings in the Yemen Arab Republic. *Applied Energy* 1986;24:245–276. [CrossRef]

[22] Aste N, Angelotti A, Buzzetti M. The influence of the external wall's thermal inertia on the energy performance of well insulated buildings. *Energy and Buildings* 2009;41:1181–1187. [CrossRef]

[23] Aste N, Leonforte, F, Manfren M, Mazzon M. Thermal inertia and energy efficiency—Parametric simulation assessment on a calibrated case study. *Applied Energy* 2015;145:111–123. [CrossRef]

[24] Argunhan Z, Oktay H, Yumrutas R. Comparison of heat gain values obtained for building structures with real and constant properties. *BEU Journal of Science* 2019;8:1518–1532. [CrossRef]

[25] Turkish Standard Number Turkish Standard Number 825 (TS 825), 1999. Official Gazette Number 23725 (in Turkish).

[26] Sisman N, Kahya E, Aras N, Aras H. Determination of optimum insulation thicknesses of the external walls and roof (ceiling) for Turkey's different degree-day regions. *Energy Policy* 2007;35:5151–5155. [CrossRef]

[27] Stock Photo – A weathered stone wall with differing size cut stone showing masonry skills in buildings. Available at: https://www.123rf.com/photo_128069620_a-weathered-stone-wall-with-differing-size-cut-stone-showing-masonry-skills-in-buildings-.html, Accessed on Oct 17, 2020.

[28] <https://ddbs.com.au/shop/bricks/claypave-regal-bricks-230x110x75-tan/>, Citation Date: 17/01/2020. Erişim adresi hata veriyor.

[29] Stock Photo – Under construction blocks wall. It is constructed with autoclaved aerated concrete. Available at: https://www.123rf.com/photo_85260554_under-construction-blocks-wall-it-is-constructed-with-autoclaved-aerated-concrete-.html, Accessed on Oct 17, 2020.

[30] Arıcı ME, Güler B. Numerical investigation of transient response of building components for the cooling process. XI. International. HVAC+R Technology Symposium, 2014, Abst. 0040.

[31] Crabb JA, Murdoch N, Penman JM. A simplified thermal response model. *Building Services Engineering Research and Technology* 1987;8:13–19. [CrossRef]

[32] Kircher KJ, Zhang KM. On the lumped capacitance approximation accuracy in RC network building models. *Energy and Buildings* 2015;108:454–462. [CrossRef]

[33] Khalilian M. Experimental investigation and theoretical modelling of heat transfer in circular solar ponds by lumped capacitance model. *Applied Thermal Engineering* 2017;121:737–749. [CrossRef]

[34] Bilgin F, Arıcı M. Effect of phase change materials on time lag, decrement factor and heat-saving. *Acta Physica Polonica A* 2017;132:1102–1105. [CrossRef]

[35] Netam N, Sanyal S, Bhowmick S. A mathematical model featuring time lag and decrement factor to assess indoor thermal conditions in low-income-group house. *Journal of Thermal Engineering* 2020;6:114–127. [CrossRef]

[36] Loveday DL, Taki AH. Convective heat transfer coefficients at a plane surface on a full-scale building façade. *International Journal of Heat and Mass Transfer* 1996;39:1729–1742. [CrossRef]

[37] Çengel YA. Heat Transfer: A Practical Approach, 2nd ed. New York: McGrawHill, 2003.

[38] Xu B, Li PW, Chan CL. Extending the validity of lumped capacitance method for large Biot

number in thermal storage application. *Solar Energy* 2012;86:1709–1724. [\[CrossRef\]](#)

[39] Jara EAR, Flor FJS, Dominguez SA, Felix JLM, Lissen JMS. A new analytical approach for simplified thermal modelling of buildings: self-adjusting RC-network model. *Energy and Buildings* 2016;130:85–97. [\[CrossRef\]](#)

[40] Gouda MM, Danaher S, Underwood CP. Building thermal model reduction using nonlinear constrained optimization. *Building and Environment* 2002;37:1255–1265. [\[CrossRef\]](#)

[41] Huang H, Zhou Y, Huang R, Wu H, Sun Y, Huang G, et al. Optimum insulation thicknesses and energy conservation of building thermal insulation materials in Chinese zone of humid subtropical climate. *Sustainable Cities and Society* 2020;52:101840. [\[CrossRef\]](#)

[42] Gagliano A, Patania F, Nocera F, Signorello C. Assessment of the dynamic thermal performance of massive buildings. *Energy and Buildings* 2014;72:361–370. [\[CrossRef\]](#)